Monodisperse Emulsion Generation via Drop Break Off in a Coflowing Stream

P. B. Umbanhowar,*,† V. Prasad,‡ and D. A. Weitz‡

Department of Physics & Astronomy, Northwestern University, Evanston, Illinois 60208, and Department of Physics, Harvard University, Cambridge, Massachusetts 02138

Received February 2, 1999. In Final Form: August 18, 1999

We describe an experimental technique for the production of highly monodisperse emulsions (with minimum achievable polydispersities <3%). The phase to be dispersed is introduced into a coflowing, surfactant-laden continuous phase via a tapered capillary. Drops detach from the capillary when the streamwise forces exceed the force due to interfacial tension. Drop size is a function of the capillary tip diameter, the velocity of the continuous phase, the extrusion rate, and the viscosities and interfacial tension of the two phases. Emulsions composed of a variety of fluids and with drop sizes ranging from 2 to 200 μm have been produced using this technique.

Introduction

An emulsion is a mixture of two immiscible liquids, one of which is dispersed in the continuous phase of the other. By contrast to microemulsions, the emulsions we consider here are thermodynamically metastable. Common emulsions include oil-in-water (O/W), or direct emulsions, and water-in-oil (W/O), or inverted emulsions. Addition of a surfactant is essential for long-term stability: the surfactant accumulates at the fluid−fluid interface and inhibits drop recombination and coarsening.[1,2] Technological applications of emulsions range from drug delivery and polymerization processing to oil recovery and hazardous material handling. Of particular interest are recent advances in the production of ordered materials with novel optical and mechanical properties by way of "emulsion templating"[3] or polymer encapsulation.[4] Emulsions with lower polydispersity produce higher quality materials in these potentially technologically important systems and are essential for some applications where ordered structures are desired.

Typically, emulsions are made by fissioning droplets with shear or impact; the resulting suspensions possess a wide size distribution of drop sizes. Distributions can be narrowed by means of a crystallization fractionation technique,[5] but the method is time-consuming, is inefficient because the bulk of the dispersed phase is not used, and produces narrow size distributions only with significant effort and skill. Techniques for the direct production of an emulsion's constituent drops include membrane extrusion,[6] microthread generation,[7] viscoelastic shear,[8,9] and driven Rayleigh jet breakup in the presence of an external liquid[10] or gas.[11,12] Experiments by Mason and Bibette[8] have shown that viscoelastic shear can yield emulsions with a polydispersity of ≈5% (standard deviation of radius divided by mean radius), but typical values for polydispersity under production conditions are ≈16%. Driven Rayleigh jet breakup consistently produces drops with size distributions narrow enough to form structures with long-range order. However, this technique also has significant limitations: minimum drop diameters are approximately twice the jet/orifice diameter, limiting the minimum size that can be produced; the jet must be actively driven at high frequencies which become difficult to implement as the drop size is decreased; if the jet velocity varies, due, for example, to orifice clogging, drop size will change and polydispersity will typically increase; finally, the jet must break up into drops before it becomes turbulent due to interaction with the ambient fluid—a surrounding gas reduces these effects but necessitates the later introduction of the drops into the continuous phase fluid.

To overcome the limitations associated with the aforementioned methods, we have developed a technique based on the flow of a surfactant-containing continuous phase past the end of a capillary through which the dispersed phase is extruded. Essentially, drops form at the tip of the capillary and then detach when they reach a size where the drag due to the coflowing liquid exceeds the interfacial tension. Advantages of this technique include the following: no external periodic forcing is required, drops are quickly coated with surfactant to form stable emulsions, production rates can be increased arbitrarily by employing additional capillaries, high volume fractions are achievable through the use of closed flows, and, as Figures 1 and 2 show, emulsions with extremely low polydispersity are produced.

Background

Drop and bubble formation at the end of a tube has been the subject of numerous investigations, many of

* To whom correspondence may be addressed. E-mail: umbanhowar@nwu.edu.

† Northwestern University.

‡ Harvard University.

(1) Becher, P. *Emulsions: Theory and Practice*; Reinhold: New York, 1965.

(2) Sebba, F. *Foams and Biliquid Foams*—Aphrons; Wiley: Chichester, 1987.

(3) Imhof, A.; Pine, D. J. *Nature* **1997**, *389*, 948.

(4) Drzaic, P. S. *Liquid Crystal Dispersions*; World Scientific: River Edge, NJ, 1995.

(5) Bibette, J. *J. Colloid Interface Sci.* **1991**, *147*, 474.

(6) See for example: Nagashima, S.; Ando, S.; Makino, K.; Tsukamot, T.; Ohshima, H. *J. Colloid Interface Sci.* **1998**, *197*, 377. Kawakatsu, T.; Komori, H.; Nakajima, M.; Kikuchi, Y.; Yonemoto, T. *J. Chem. Eng. Jpn.* **1999**, *32*, 241.

(7) Gañán-Calvo, A. M. *Phys. Rev. Lett.* **1998**, *80*, 285.

(8) Mason, T. G.; Bibette, J. *Langmuir* **1997**, *13*, 4600.

(9) Perrin, P. *Langmuir* **1998**, *14*, 5977.

(10) Timm, E. E.; Leng, D. E. U.S. Patent Number 4,623,706, 1986.

(11) Timm, E. E. U.S. Patent Number 4,444,961, 1984.

(12) For a description of driven jet breakup see for example: Berglund, R. N.; Liu, B. Y. H. *Environ. Sci. Technol.* **1973**, *7*, 147. Ström, L. *Rev. Sci. Instrum.* **1969**, *40*, 778.

10.1021/la990101e CCC: $19.00
Published on Web 10/14/1999

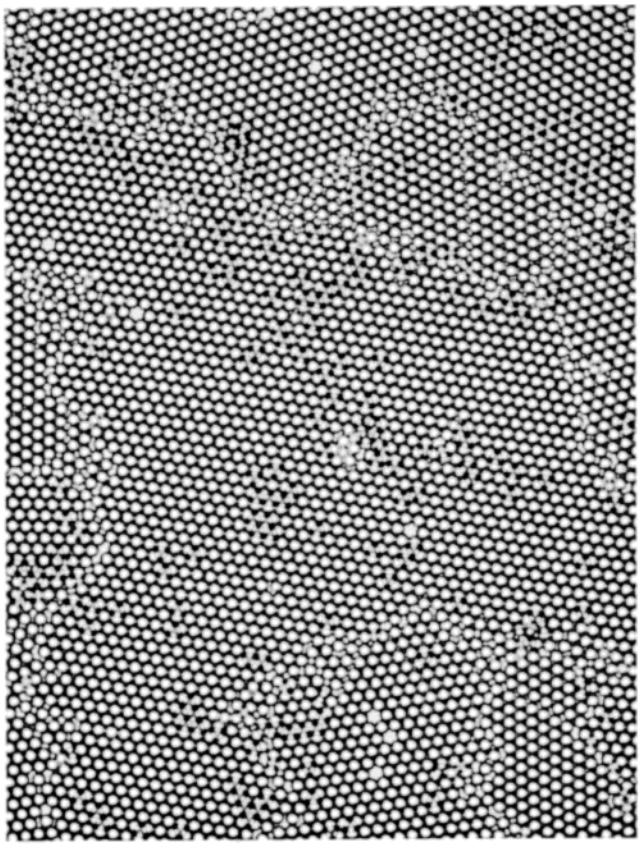

Figure 1. Monolayer formed from a 10 μm diameter monodisperse emulsion of silicone oil in water ($d_i = 5$ μm, $v = 38$ cm/s). Vacancies (larger bright regions), double layers (darker regions), and grain boundaries are evident.

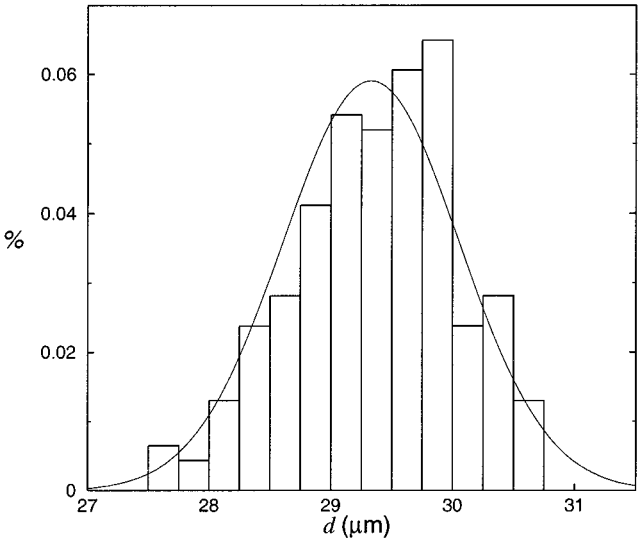

Figure 2. Normalized diameter distribution for silicone oil in water emulsion obtained using video microscopy ($d_j = 9.7$ μm, $v = 151$ cm/s). Solid line is a Gaussian fit with $\sigma/d = 0.03$.

which are summarized in Clift.[13] The majority of studies have focused on conditions where buoyancy is the primary mechanism driving drop separation.[14,15] A few studies examined the effect of an external flow, but only for the case of the formation of gas bubbles in liquid.[16,17] Liquid–liquid drop formation has been examined by Scheele and Meister, but only for the case of a quiescent continuous phase.[18] A recent numerical investigation by Zhang and Stone examined drop formation for fluids of arbitrary viscosity and density, where both buoyancy and external fluid flow are considered.[19] However, for our technique a simple model of drop break off,[14,17,18] proves adequate for a basic understanding. In the initial stage (growth), the net force on the drop is near zero and the drop remains essentially spherical, as shown in Figure 3a. In the second stage (separation), a neck forms and eventually breaks as the drop leaves the tip (Figure 3b).

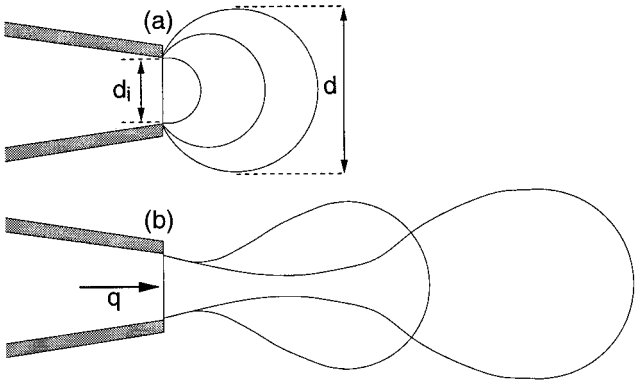

Figure 3. Stages of drop evolution: (a) growth, (b) separation.

For stable drop growth at the tip, the inner fluid flow rate, q, must be low enough that a jet does not develop when the dispersed fluid exits the tube. A lower bound for when jetting will occur as a function of q is obtained by equating the kinetic energy per unit length $\rho_d \pi d_i^2 v_j^2/8$ with the surface energy per unit length $\pi d_i \gamma$, where ρ_d is the dispersed phase density, d_i is the tube inner diameter, v_j is the jet velocity, and γ is the interfacial tension. Jetting will not occur as long as $q < \pi(d^3\gamma/2\rho_d)^{1/2}$. This is a conservative estimate since dissipative effects of the continuous phase are neglected. However, for the majority of conditions the factor limiting the flow rate is not jetting but rather the requirement that the spacing between drops be greater than a minimum of $O(d)$.

In the absence of jetting, drops grow spherically from the capillary tip until the net force acting on the drop exceeds zero and separation begins (see Figure 3). The details surrounding the separation phase are complicated[19,20] and are not adequately described by models which consider the detaching drop as a simple sphere. However, a brief discussion of the forces acting on a spherical drop is useful for understanding the gross behavior of the emulsion generator. The interfacial tension force, which holds the drop on the tube, is $\pi d_i \gamma$. However, the actual perimeter of the triple interface is likely to be somewhere between πd_i and πd_o, where $d_o \approx 1.5 d_i$ is the tip outer diameter.[17] The drag force in the limit of low Reynolds number ($\mathrm{Re} = d v \rho_c/\eta_c$) is given by a modified version of the Stokes formula $3\pi\eta_c(d - d_o)(v - v_d)$, where η_c, v, and ρ_c are respectively the dynamic viscosity, velocity, and density of the continuous phase, d is the drop diameter, and $v_d \approx q/\pi d^2$ is the streamwise velocity component of

(13) For a summary see: Clift, R.; Grace, J. R. Weber, M. E. *Bubbles, Drops, and Particles*; Academic: New York, 1978.
(14) Heertjes, P. M.; de Nie, L. H.; de Vries, H. J. *Chem. Eng. Sci.* **1971**, *26*, 441.
(15) Longuet-Higgins, M. S.; Kerman, B. R.; Lunde, K. *J. Fluid Mech.* **1991**, *230*, 365.
(16) Oğuz, H. N.; Prosperetti, A. *J. Fluid Mech.* **1993**, *257*, 111.
(17) Chuang, S. C.; Goldschmidt, V. W. *Trans. ASMED: J. Basic Eng.* **1970**, *92*, 705.
(18) Scheele, G. F.; Meister, B. J. *AIChE J.* **1968**, *14*, 9.
(19) Zhang, D. F.; Stone, H. A. *Phys. Fluids* **1997**, *9*, 2234.
(20) Shi, X. D.; Brenner, M. P.; Nagel, S. R. *Science* **1994**, *265*, 219.
(21) Mason, T. G.; Lacasse, M.; Grest, G.; Levine, D.; Bibette, J.; Weitz, D. A. *Phys. Rev. E* **1997**, *56*, 3150.

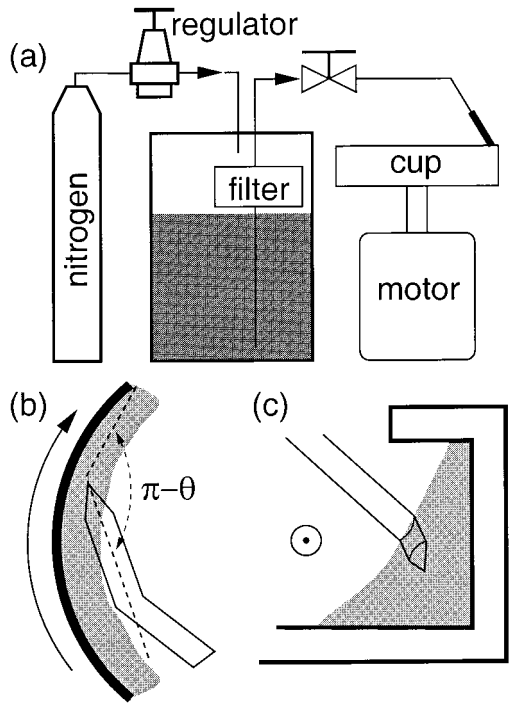

Figure 4. (a) Schematic of experimental setup and (b, c) details of tip/fluid contact geometry.

the expanding drop. The term $d - d_o$ accounts for the shielding of the drop from the continuous phase by the tip, while the term $v - v_d$ reflects the reduction in the relative velocity between the continuous phase and the drop due to the growth-induced motion of the drop away from the tip (see Figure 3a). The expression for the drag is not exact—the modified terms are at best approximate, the Stokes formula is only valid for Re ≤ 1, whereas Re for the data presented here ranges between 0.1 and 100, and the orientation of the tip is not parallel to $\hat{v}$. The buoyancy force is $\pi d^3 g \Delta\rho/6$, where $\Delta\rho$ is the density difference of the two phases and g the acceleration due to gravity. For $d > d_i$, the Laplace pressure produces a force of $\pi\gamma d_i^2/d$. Finally, momentum transfer from the disperse phase as it exits the capillary and enters the drop produces a force of $4\rho_d q^2/\pi d_i^2$.

For the parameters used here, the buoyancy, Laplace pressure, and momentum transfer terms are all small in comparison to the viscous drag and are ignored. Balancing the surface tension with the viscous drag and using the nondimensionalized variables $\tilde{v} = v/v_o$, $\tilde{d} = d/d_i$, and $\tilde{q} = q/q_o$ with $v_o = \gamma/3\eta_c$ and $q_o = \pi d_i^2\gamma/3\eta_c$ yields

$$\tilde{v}\tilde{d}^3 - (\tilde{v} + 1)\tilde{d}^2 - \tilde{q}\tilde{d} + \tilde{q} = 0 \qquad (1)$$

where we have assumed that $d_i \approx d_o$. This equation describes the basic mechanism of the drop formation. Note, however, that eq 1 does not account for fluid transfer to the drop during separation.

Experiment

Figure 4 shows a schematic diagram of the experiment. A 4-cm-radius Teflon cylindrical cup with a flat bottom and a small top lip is attached to a speed-controlled motor and partially filled with the surfactant containing continuous phase. The cup is rotated at constant angular velocity, and the fluid quickly achieves solid body rotation, collecting on the side in the well formed by the lip. The conical tip of a small glass tube (0.1 cm outer diameter), bent at ≈45° to facilitate placement, is immersed in the continuous phase at an angle $\theta \approx 30°$ with the free surface. The other end of the tube is connected to a pressure-regulated dispensing vessel containing the dispersed phase. The dispersed phase is passed through a 0.1 μm filter before leaving the dispensing vessel to prevent clogging. Tip inner diameters are $0.7 < d_i < 100$ μm, and tips are prepared using a pipet puller or are purchased from a commercial source. For the O/W emulsions described here, we use sodium dodecyl sulfate (SDS) dispersed in the continuous phase as a surfactant. The physical properties of the dispersed phase liquids at room temperature are listed in Table 1.

Table 1. Physical Properties for Dispersed Phases

liquid	ρ (g/cm^3)	η (cP)	γ (dyn/cm)[a]
silicone oil (PDMS[b])	0.937	12	9.2
hexadecane	0.773	3.3	4.9
liquid crystal	1.05	37	9.3

[a] With 8 mM SDS in H_2O. [b] Polydimethylsiloxane.

Video microscopy is used to measure both drop and tip diameters. Measurements of interfacial tension are obtained using the pendant drop technique. A minor complication resulting from our free surface geometry is the large evaporation rate of the continuous phase, which increases with rotation velocity, necessitating the use of a fluid level control system for runs of significant duration. In addition, enhanced evaporation causes significant cooling of the continuous phase—temperatures low enough to freeze hexadecane (a fluid used in this study) are possible depending on ambient temperature and humidity. Although the dispersed fluid is delivered under constant pressure conditions, we consider the flow rate to be constant as well, since the supply pressure is significantly larger than the maximum internal drop pressure. Also, we assume that the viscosity of the continuous phase (water) is 0.01 P and independent of surfactant concentration.

Results

Figure 1 is an image of an emulsion in which drops have floated to the surface and formed monolayer crystalline domains. The long-range order demonstrates the extremely low polydispersity which is achievable using this technique. As Figure 1 shows, no visible satellites or larger drops formed by drop coalescence are present. In general, satellite drops are observed only occasionally, and when present, their diameter is no larger than 0.1 of the primary drop diameter; thus they can easily be separated from the primary drops. Figure 2 shows a probability distribution of the drop size. Drop diameters are determined from digital images by measuring the area contained within equal intensity contours—a technique that is sensitive to inhomogeneous lighting conditions and leads to an increase in the apparent polydispersity. Despite inhomogeneous lighting, this analysis of Figure 2 indicates that polydispersities of less than 3% can be achieved.

To consider the mechanism of drop formation, we show in Figure 5 a plot of drop diameter versus outer flow velocity for a typical run. The drop diameter is a decreasing function of velocity and can be varied by more than a factor of 4. Control of the outer flow velocity allows precise selection of drop size. It also provides a simple mechanism for production of bidisperse or multidisperse drop size distributions. When $\tilde{q}$ is small, eq 1 reduces to

$$\tilde{d} = 1 + \tilde{v}^{-1} \qquad (2)$$

The solid line in Figure 5 is a fit to this functional form

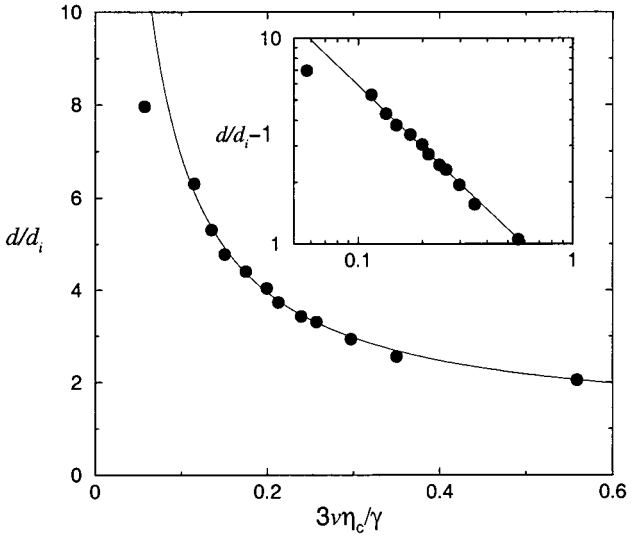

Figure 5. Drop diameter versus outer flow velocity for hexadecane in water emulsion ($d_i = 16$ μm, $c = 16$ mM SDS, $\eta_c = 0.01$ P, $\gamma = 9$ dyn cm^{-1}, and $q \approx 10^{-6}$ cm^3 s^{-1}). Solid curve is a fit to $d/d_i = 1 + a/\tilde{v}$ with $a = 0.6$. Inset shows the same data on a log−log scale.

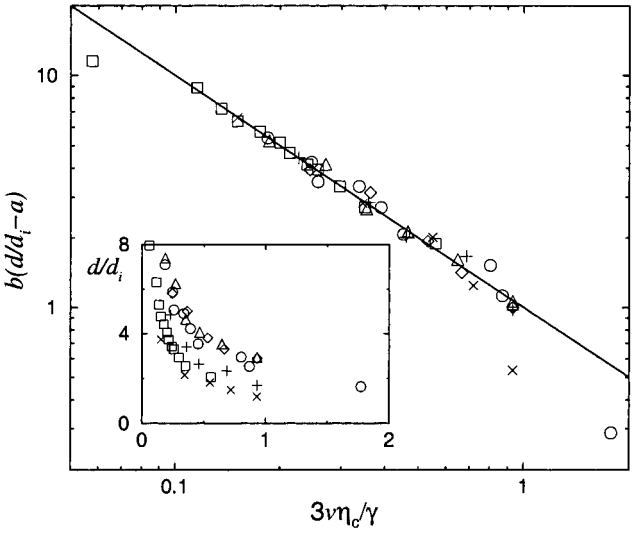

Figure 6. Drop diameter scaled by a and b vs outer flow velocity for hexadecane in water emulsion, where a and b for each data set are fit to $d/d_i = a + b/\tilde{v}$. The solid line is a plot of $d/d_i = 1 + 1/\tilde{v}$. Inset shows the unscaled data (○, $d_i = 5.8$ μm, $a = 1.3$, $b = 1.1$; □, $d_i = 16$ μm, $a = 0.9$, $b = 0.6$; ◇, $d_i = 3.8$ μm, $a = 1.9$, $b = 1.0$; △, $d_i = 4$ μm, $a = 1.8$, $b = 1.1$; +, $d_i = 9$ μm, $a = 0.8$, $b = 0.9$; ×, $d_i = 11.5$ μm, $a = 1.0$, $b = 0.5$; $c = 16$ mM SDS for all sets).

with $\tilde{v}$ scaled by 0.6. The necessity of introducing a fit parameter is most likely due to an increase in the local flow velocity around the tip caused by the finite angle between the tip and the fluid and the underestimation of the drag force by the Stokes formula (Re > 5). The obvious deviation of the lowest velocity data point from the fit is attributable to the neglect of buoyancy.

The dependence of drop diameter on v for six different d_i is shown in Figure 6. As the inset indicates, noticeable offsets exist between the scaled data sets. However, when each data set is fit to $d/d_i = a + 1/b\tilde{v}$ and then plotted as $b(d/d_i - a)$ versus $\tilde{v}$, good collapse that is well characterized by eq 2 is achieved. Despite variations in the angle between the capillary tube and the fluid for runs with different d_i ($20° < \theta < 40°$), uncertainties in the effective interface length, and changes in the effective drag coefficient (i.e., $0.1 < \mathrm{Re} < 25$), a and b for the different tip sizes are all close to 1 (see caption of Figure 6).

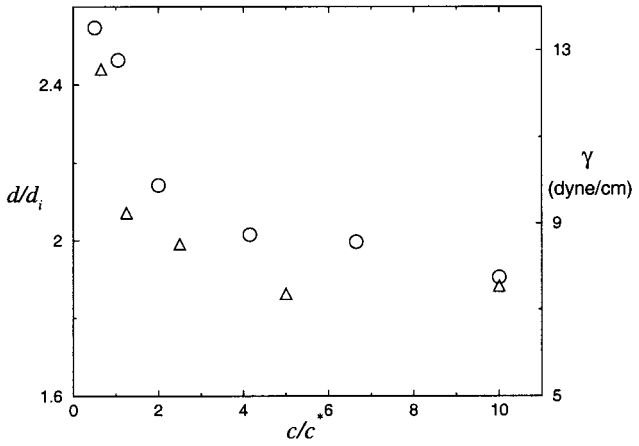

Figure 7. Dependence of drop diameter (○) and surface tension (△) on SDS concentration for silicone oil ($d_i = 10.7$ μm, $v = 120$ cm/s, $q = 4 \times 10^{-6}$ cm^3/s).

Figure 7 shows the dependence of d and γ on surfactant concentration c with v and q fixed. Above the critical micelle concentration for SDS ($c^* = 8$ mM), there is little change in the drop diameter or γ.[22] As c decreases, d and γ increase similarly as would be expected from eq 2. For $c < 0.1c^*$, monodisperse emulsions are not formed, most likely as a result of drop coalescence due to inadequate surfactant coverage. In addition to depending on c, the surface tension of a newly created interface in the presence of a surfactant is also a decreasing function of time. However, the measurements of this time dependence, of which we are aware, are performed under conditions where diffusion, and not advection as is the case in our experiments, is the dominant mechanism for transporting surfactant from the bulk to the interface.[23,24] The good agreement between the calculated and measured drops sizes supports a near saturation of the interface on a time scale on the order of the drop formation time, which is 10^{-2}−10^{-5} s for our experiments. This is in contrast to the case of diffusion-dominated transport where saturation times are about 100 s.

Finally, in addition to depending on v, d_i, and γ, the drop diameter is also a function of q as Figure 8 shows. Note that d is approximately doubled when q is increased by a factor of 10. The q-dependent terms in eq 1 are too small to account for this change. Similar behavior is observed in simulation[19] and in experiment with gas bubbles.[16] As noted earlier, drop formation includes a separation stage during which the drop moves away from the tip but remains connected to the tip by a neck. Simulations show that drops are highly elongated and that the separation times are large when the viscosity ratio η_d/η_c is greater than 1.[19] For the fluids used here $\eta_d/\eta_c > 3$. Thus, we believe it is likely that the dependence of d on q arises from fluid transfer during separation. Further experiments that visualize the drop break-off process should help clarify this behavior.

Discussion

Monodisperse emulsions with diameters $2 < d < 200$ μm have been produced using a drop break-off technique.

(22) Evans, D. F.; Wennerstrom, H. *The Colloidal Domain: where Physics, Chemistry, Biology and Technology meet*; VCH Publishers, Inc.: New York, 1994.

(23) Campanelli, J. R.; Wang, X. *J. Colloid Interface Sci.* **1997**, *190*, 491.

(24) Bonfillon, A.; Sicoli, F.; Langevin, D. *J. Colloid Interface Sci.* **1994**, *168*, 497.

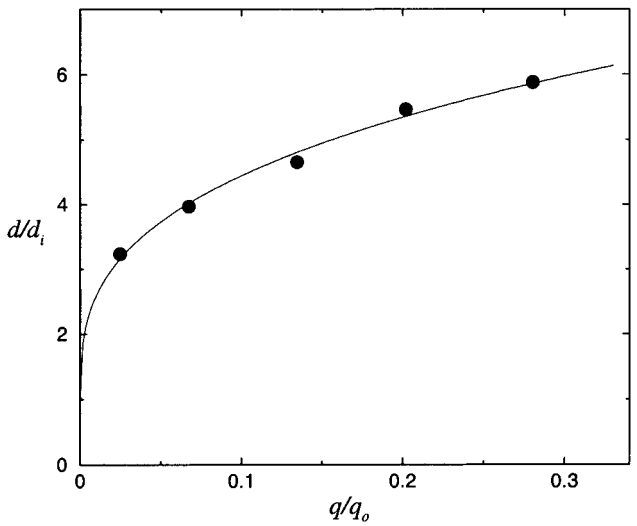

Figure 8. Drop diameter versus volumetric flow rate for PDMS in water emulsion ($d_i = 4\ \mu$m, $v = 118$ cm/s, $c = 16$ mM). Solid curve is a fit to $d/d_i = a + b(q/q_o)^{1/3}$ with $a = 1$ and $b = 19$.

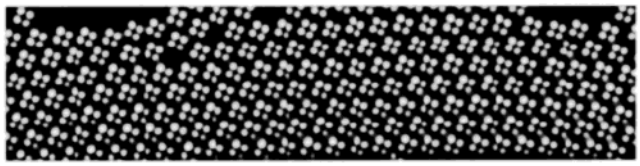

Figure 9. 5 μm liquid crystal emulsion viewed between crossed polarizers.

In addition to hexadecane, PDMS, and liquid crystal, emulsions have been made with dispersed phases of hexane and mineral oil. Emulsions have also been prepared using dispersed phases composed of mixtures of ether and liquid crystal (see Figure 9), ether and PDMS, isooctane and hexadecane, and isooctane and PDMS. Addition of ether to the internal phase reduces its viscosity, facilitating extrusion through small diameter tips; the ether also will evaporate after the drops form, allowing even smaller final drop size to be achieved. Continuous phases of water and glycerol mixtures have also been used successfully. A single attempt to produce a W/O emulsion with hexadecane as the continuous phase and Span 80 as a surfactant proved unsuccessful due, most likely, to the hydrophilic surface of the glass capillary. In retrospect, this is not surprising since the successful production of emulsions via membrane extrusion requires that the dispersed phase not wet the extruding surface.[25] Our technique can clearly be generalized to other systems where the steady mean flow past the tip is generated by other means and where different surfactants and liquids are used.

Two hurdles exist for the production of submicrometer drops, both of which are practical. First, as the tip size decreases the probability that the tip will clog or narrow increases. For our apparatus, difficulties are encountered for tip diameters less than about 1 μm. The use of electron microscope grade liquids combined with careful cleaning procedures would do much to alleviate these difficulties. The other, more important limitation, is one of production rates. Since drops are produced in a line, the volume production rate will scale as vd_i^2. Adding more tips to increase the production rate is only practical if variations in tip size are less than the minimum required polydispersity. Nevertheless, barring tip clogging, laboratory-scale production rates of small drops are feasible; for example, about 1 cm^3 a day of 5 μm diameter drops at 50% volume fraction can be produced with a single tip. This compares well with other techniques, such as fractionated crystallization, which are also very time-consuming. For the production of large drops, there are three limiting factors. First, for larger drops the flow around the drop becomes turbulent, producing velocity fluctuations that will cause variations in drop size. Second, the Laplace pressure becomes negligible leaving the drops vulnerable to tearing due to velocity gradients. Finally, as the drops get larger the buoyancy term, which scales as d^3, begins to dominate. In the limit of large drops, it is probably more practical to drive drop separation entirely by gravity in the absence of an external flow or to use other methods.

Summary

We have developed a simple technique for the production of highly monodisperse emulsions. Drag forces generated by a coflowing, surfactant-laden continuous phase detach drops of the dispersed phase from the end of a small tube. The method is easily scalable since the tips from which the drops are produced are passive. By variation of the velocity of the continuous phase, precise control of the emulsion size is achieved. Emulsions are stable and contain few satellite drops even when fluids with high viscosity ratios are used. Finally, a simple model predicts the size of the resulting emulsions for varying v, d_i, and γ.

Acknowledgment. This work was supported by NASA (NAG3-2058) and by the Materials Research Science and Engineering Center program of the NSF under award DMR 96-32539.

LA990101E

(25) See for example: Kandori, K. In *Food Processing: Recent Developments*; Gaonkar, A. G., Ed.; Elsevier: New York, 1995; Chapter 7.